Broadband dynamic spectrum characterization based on gating-assisted electro-optic time lens

View Online   Export Citation   CrossMark

Yuan Wei,[a)] (iD) Bowen Li,[a),b)] Pingping Feng, Jiqiang Kang, and Kenneth K. Y. Wong[b)] (iD)

AFFILIATIONS

Department of Electrical and Electronic Engineering, The University of Hong Kong, Pokfulam Road, Hong Kong, China

[a)] **Contributions:** Y. Wei and B. Li have contributed equally to this work.
[b)] **Electronic addresses:** bwli@eee.hku.hk and kywong@eee.hku.hk

ABSTRACT

A broadband real-time optical spectrum characterization technique is proposed based on a gating-assisted electro-optic time lens. Operating at the repetition rate of 10-MHz, a 10-dB spectral measurement range of more than 70-nm is achieved with a resolution of up to 42.5-pm in the near-infrared regime. To demonstrate its performance in applications, real-time spectral observation of broadband wavelength sweeping of a Fourier domain mode-locked laser and a 32.4-GHz optical frequency comb is presented. Furthermore, a detailed comparison between dispersive Fourier transform and the time lens based spectral analysis technique for frequency comb measurements is made from both simulation and experiment. With its broadband performance, this technique can provide widespread applications requiring real-time spectral analysis.

Published under license by AIP Publishing. https://doi.org/10.1063/1.5079424

Optical spectroscopy is of great merit in broad research areas by serving as the basic instrument for both fundamental and applied sciences.[1–3] Apart from characterizing stationary and deterministic scenarios, optical spectrometers are also highly desired to operate in real-time to trace the transient and non-repetitive dynamics. As one of the most prevailing and powerful tools of real-time spectral analysis, dispersive Fourier transform (DFT)[4–6] has profoundly facilitated the ultrafast dynamics study in optical physics.[7–9] By using chromatic dispersion, the DFT temporally stretches the signal under test (SUT) and encodes the SUT's spectral profile onto its temporally broadened waveform. Thanks to its elegant simplicity, the DFT technique can be easily applied and hence has served as one of the standardized spectral analysis solutions for ultrashort optical pulses. However, DFT implementation is required to satisfy the temporal Fraunhofer (far-field) condition for the output waveform envelope to resemble the Fourier transform of the input signal.[10,11] Therefore, a waveform of an arbitrarily dispersed pulse cannot guarantee to represent its spectral profile in the time-domain. This prerequisite for DFT inherently limits its scope of application. On the other hand, it is well established that a time lens (TL) can perform optical Fourier transform according to the space-time duality.[12,13] Proposal of this concept dates back to 1983,[14] and its first experimental demonstration

was made using a phase modulator (PM).[15] However, as it lacked an independent control of the repetition rate, the system inevitably operated at the frequency of sinusoidal phase modulation and hence only supported a heavily limited spectral measurement range of below 1nm. Recently, such a concept has also been applied to the real-time Fourier analysis in radio frequency (RF),[16] whereas it serves a different purpose of distinguishing RF tones with a MHz frequency difference. To enable the broadband real-time optical spectrum analysis in applications, a parametric spectro-temporal analyzer (PASTA), where a time lens is created by an optical parametric process, has been demonstrated and further upgraded to provide a 30 nm spectral measurement range.[17–20] However, owing to the nature of the optical parametric process, these parametric based spectrometers must function at wavelengths where phase matching can be readily satisfied. This requirement not only inherently refrains their applicability but also imposes ultimate restriction on the achievable spectral measurement range.

To overcome these drawbacks of the parametric based time lens, a broadband real-time spectral analyzer based on a gating-assisted electro-optic (EO) time lens is reported in this work. The system's operating principle is shown in Fig. 1. A programmable time gate created by an amplitude modulator (AM) is placed right before the time lens to function as a time aperture.
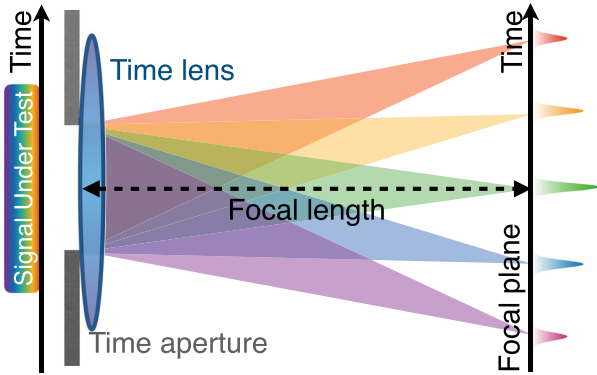
FIG. 1. Operating principle of the proposed system.

FIG. 2. (a) Experimental setup. (b) AWG pattern and the experimentally measured electrical gate waveform after the RF amplification for driving AM. (c) AWG pattern and the experimentally measured electrical parabola waveform after the RF amplification for driving PM, in comparison with the theoretical parabola and sinusoidal curves. (d) The recorded optical waveforms at the AM output (red) and the system output (blue), respectively. (e) Characterization of the 10-dB spectral measurement range when the signal wavelength was tuned from 1528 nm to 1600 nm at a step of 4-nm. Inset: the wavelength-to-time mapping curve. SOA, semiconductor optical amplifier; AWG, arbitrary waveform generator; PC, polarization controller; AM, amplitude modulator; PM, phase modulator; WDMC, wavelength-division-multiplexing coupler; and DCF, dispersion-compensating fiber.

A time lens, created by a phase modulator (PM), performs optical Fourier transform of the gated input signal, by focusing different optical frequency components onto different temporal locations in the focal plane. Equipped with the time gate, this system features independent repetition-rate control and thus supports a much broader spectral measurement range where the system's repetition rate is required to be inversely decreased. Compared with its parametric time-lens counterparts, this EO system is much more wavelength-flexible and can be easily implemented in spectral regimes wherever the EO modulators are commercially available. With its versatility, the proposed system can offer real-time spectral detection for various applications requiring broadband analysis and effectively complement the parametric spectrometers in the spectral regimes where phase matching is hard to realize.

The experimental setup is shown in Fig. 2(a). The input signal is amplified by a semiconductor optical amplifier (SOA) and then enters the AM (time gate). After the time gate, the gated light is injected into a PM (time lens). Two polarization controllers (PCs) are employed right before the two EO modulators to manipulate the polarization states of the incident light. Specifically, the focal length of the time lens is set to equal the group delay dispersion (GDD) of the dispersion-compensating-fiber (DCF). After the PM, the modulated light propagates through the DCF for temporal focusing and is compressed to be transform-limited pulses at the DCF output. The DCF provides a GDD of 1693-ps^2 at 1545-nm with an ultralow dispersion slope of 0.53-ps/nm^2, which enables simultaneous optimum temporal focusing for different wavelength components. In addition, to compensate the transmission loss of the DCF and further enhance the system's sensitivity, dual-Raman pumping (at 1455-nm and 1480-nm, respectively) is employed and coupled with DCF to provide broadband distributed Raman amplification (DRA) along the DCF.[21] The gain provided by the DRA was 16-dB at 1550-nm and can vary from 12 to 16 dB across the whole 70-nm wavelength range.

In the experiment, the implementation of the time gate and the time lens is realized by imparting the amplified electrical waveform patterns from two synchronized output channels of an arbitrary waveform generator (AWG, Tektronix AWG70000A)
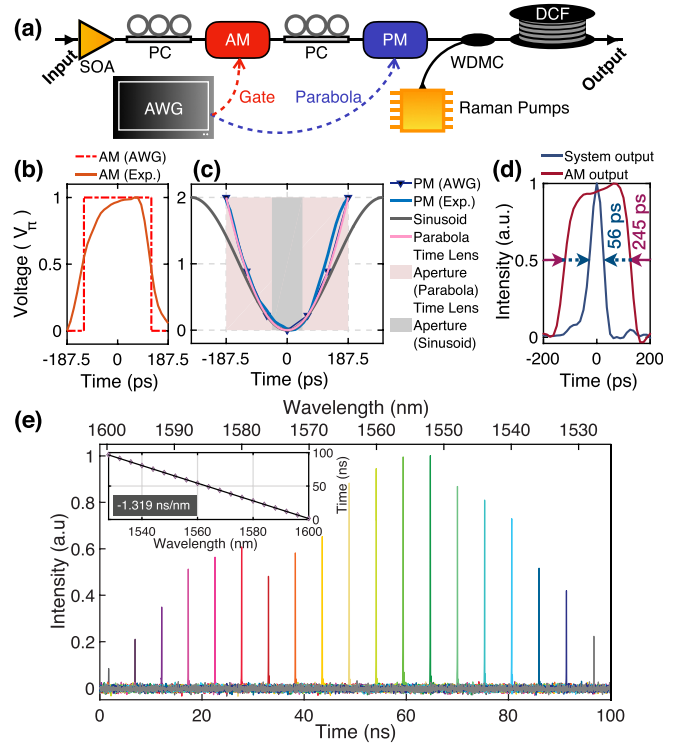
to the EO modulators. In particular, the AWG's internal clock was applied to both of the output channels for the purpose of waveform pattern synchronization. Mathematically, the time lens is a quadratic phase shift. Experimentally, this quadratic phase shift was applied by a parabolic pattern directly generated from the AWG. Compared with the previous method of mitigating the phase aberration of a sinusoid-driven EO time lens,[22] our quadratic implementation directly creates a theoretically aberration-free time lens with only one phase modulator, which not only serves the same purpose but also brings conceptual and practical simplicity. Furthermore, instead of deliberately introducing a phase-lock loop to stabilize the repetition rate in the all-optical systems,[23,24] the proposed system fully utilizes the superb electrical stability (0.4-ps root-mean-square jitter between the time gate and the time lens patterns) of the AWG to achieve the temporal stability of the proposed system with substantial implementation simplicity. The AWG patterns of AM and PM and the corresponding amplified electrical waveforms are shown together in Figs. 2(b) and 2(c). The experimental

waveforms were measured at the output of RF amplifiers by using an 80-Gs/s real-time oscilloscope. Owing to the limited bandwidth of the electrical amplification, the parabola pattern of AWG output was low-pass filtered by the RF amplifier. Fortunately, this low-pass filtering significantly mitigates the experimental imperfection of the parabola pattern under the digitization of limited sampling and thus yields an electrical waveform of a smoother and more accurate parabola shape. Given the fixed focal length and the phase modulation depth of 2π, the details to design the electrical waveform pattern for driving a PM to produce a time lens can be found in Ref. 13. We note that a PM with low V_π performance is highly favored for the time lens implementation as it is capable of providing a larger modulation depth and hence a stronger time lens focusing. Although theoretically the time lens aperture is 100% of a parabola's temporal span, only ∼60% is found to be effective in the experiment. This is due to the experimental imperfection of time lens induced by the AWG's digitization at the limited sampling rate of 16-Gs/s and the electrical distortion during the RF amplification of the AWG pattern. This instrument-induced limitation can be significantly alleviated by simply using a more advanced AWG with a higher sampling rate (i.e., a 50-Gs/s AWG would render a $3\times$ sampling improvement). Based on the sinusoid-parabola-approximation $(V = \cos t \approx 1 - t^2/2, \; |t| \leq 1/2$, where t is the temporal coordinate and V is the modulation voltage), the ratio of temporal span between a single-cycle sinusoid $(-\pi \leq t \leq \pi)$ and its corresponding parabola $(-2 \leq t \leq 2)$ under the same modulation voltage range $(-1 \leq V \leq 1)$ is given by $(2\pi/4)$. However, only $1/2\pi$ of a sinusoid period can be effectively approximated as a parabola.[13] Therefore, if a sinusoidal cusp is used to produce a localized parabola drive under the identical experimental setting (phase modulation depth and focal length), the corresponding time-lens aperture is merely 1/4 of a parabola's temporal span and hence unable to compete with the time-lens performance enabled by the direct parabola implementation via AWG. In this regard, our direct parabola implementation suggests great potential for realizing the distortion-free time lens.

To block the unwanted incident light that falls out of the effective time window of quadratic phase modulation, the width of the time gate is hence set to 250-ps, which corresponds to the temporal record length of the SUT that participates in the optical Fourier transform in each measurement. By launching a continuous wave (CW) into the system, the system's temporal focusing can be characterized. Figure 2(d) shows the recorded optical waveforms at the AM output (red) and the system's output (blue), respectively. The time gate tailored the incident CW into a square pulse of 245-ps, and temporal focusing further compressed this square pulse into a near transform-limited pulse of 56-ps, which manifests the system's impulse response. The maximum repetition rate of AM is determined by the minimum time window size at the system output that can avoid temporal overlapping between the adjacent measurements. Here, the time window size is set to around 100-ns, which renders a system's repetition rate of 10-MHz. Depending on the spectral bandwidth of interest, the system's repetition rate can be accordingly adjusted by simply modifying the AM's repetition

rate while the time gate width remains fixed, to fit into specific application scenarios.

To quantify the spectral measurement range of the system, CW from a tunable laser was used as the input signal. The wavelength of the CW input was continuously tuned from 1528-nm to 1600-nm at a step of 4-nm, and the corresponding waveforms recorded by a real-time oscilloscope were overlapped together as shown in Fig. 2(e). The system exhibited a non-uniform wavelength responsivity as observed in the envelope of the waveform, which is mainly attributed to the spectral response of the EO modulators and the spectral gain profile of the SOA and the DRA. This roll-off envelope of the wavelength-dependent responsivity in Fig. 2(e) can be used to calibrate the measurement results to reconstruct the precise spectral shape of the input signal in the applications. Overall, the 10-dB measurement bandwidth can cover more than 70-nm, which can be further extended to 100-nm by employing multiple Raman pumps with optimized pumping strength.[25] The wavelength-to-time mapping is depicted in the inset figure, and its linear fitting shows a mapping ratio of −1.319 ns/nm. Together with the impulse response pulse width in Fig. 2(d), the spectral resolution of the system can be calculated as 56 (ps)/1.319 (ns/nm) ≈ 42.5 pm. Here, a single-wavelength CW was used as the optical input signal to quantify the system's sensitivity. It has been verified that the system's sensitivity is −20 dBm, as it is determined by the minimum input power requirement of the SOA used in the experiment. By replacing the SOA with an erbium-doped fiber amplifier (EDFA), the sensitivity can be enhanced to −32.2 dBm [slightly higher than that (−30 dBm) of the conventional PASTA system[17]], whereas the SOA was adopted here owing to its capability of broadband amplification.

To demonstrate its performance in applications, a dynamic spectral observation of lasing wavelength sweeping of a Fourier domain mode-locked laser (FDML)[26] operating at 50-kHz is presented. Figure 3 shows the reconstructed 3D spectro-temporal pattern measured by the system with the repetition rate of 10-MHz. From a practical point-of-view, this spectral-temporal observation can be used to identify the lasing wavelength in real-time and calibrate the time window of the linear wavelength sweeping regime for optimizing the imaging performance in optical coherent tomography (OCT).[27]

Furthermore, a consecutive spectral measurement of a 32.4-GHz frequency comb is demonstrated. The 32.4-GHz comb was obtained by using an optical bit-rate multiplexer to multiply the comb spacing of a home-made 8.1-GHz comb source four times. Accordingly, the time gate of 250-ps would capture 8 comb pulses in every acquisition to obtain a comb spectrum in each frame. Figure 4(a) shows two time-averaged optical spectra measured by a commercial optical spectral analyzer (OSA) over 5-s and an 80-Gs/s real-time oscilloscope at the system output averaged over 5−μs. The time axis of the recorded temporal waveforms by a real-time oscilloscope was converted to wavelengths to construct the oscilloscope measured spectrum. We note that since the comb-spacing multiplication using the commercial optical bit rate multiplexer is wavelength-dependent, not every original 8.1-GHz comb line over the entire spectral range could be optimally converted simultaneously. Therefore,
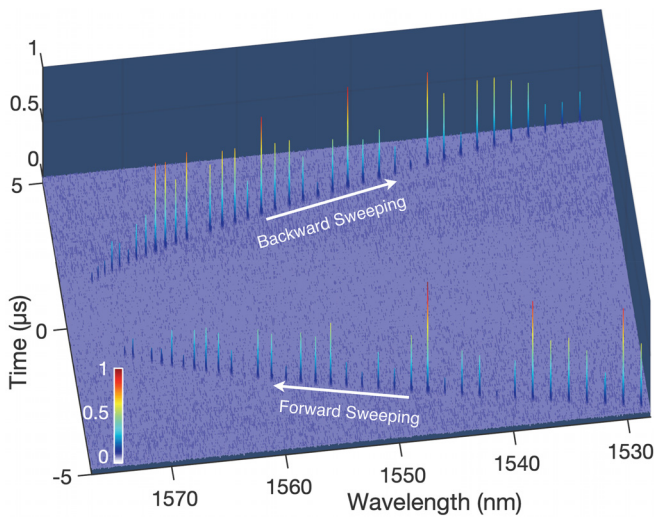
FIG. 3. 3D spectro-temporal pattern of FDML's lasing wavelength sweeping measured by the system.

there are a few residual 8.1-GHz comb lines located among the 32.4-GHz comb. Figure 4(b) presents the consecutive spectral observation over 100-μs at a frame rate of 10-MHz. Although the frequency combs in the steady state was observed here as the proof-of-concept demonstration, we expect this real-time spectral characterization to be applied to capture and analyze the transient comb dynamics that previously cannot be directly observed.[28–31]

One may consider the feasibility of using dispersive Fourier transform, assisted by the time gate, to perform real-time spectral analysis on frequency combs. Given the existing setup, the dispersive Fourier transform can be easily realized in the system by simply removing the time lens. Therefore, we applied and closely compared these two methods by only turning on/off the time lens in both experiment and simulation. Given the fact that the non-uniform experimental spectrum of our comb source is difficult to be incorporated into the simulation, for the ease of demonstration, we instead use frequency combs of identical comb spacing but with a different spectral envelope (a Gaussian-shape) as the system input in our simulation. Figures 5(a) and 5(b) show the simulated original temporal waveform and the spectrum of the 32.4-GHz comb pulses before the time gate. Fig. 5(c) presents both the experimental observation and simulation results at the system output. Notably, substantially different temporal waveforms are observed when the time lens is turned on and off. From the experiment, it is obvious that in the presence of the time lens, comb lines are clearly identified as isolated sharp pulses in the time-domain (pink line in Fig. 5). When turning the time lens off, a bunch of complicated dual-peak temporal patterns (red line in Fig. 5) consequently appeared at the system output. This experimental observation of two different waveform structures is further confirmed by the simulation. Particularly, the discrepancy in the waveform patterns between the simulation and the experiment with the time lens turned off is due to the limited bandwidth of the photodetector used in the
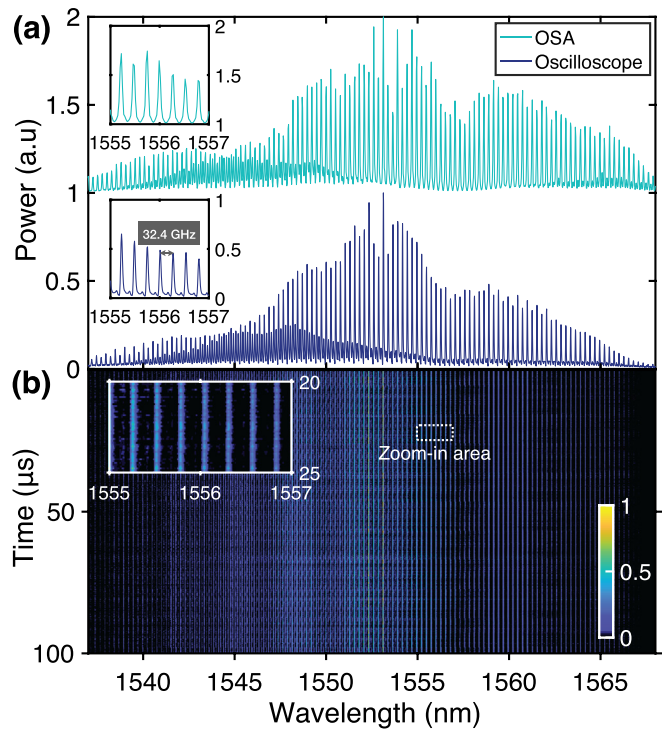

FIG. 4. Experimental measurement of a 32.4 GHz frequency comb. (a) Time-averaged comb spectra measured by OSA (green) over 5-s and by a real-time oscilloscope (blue) over 5-μs, respectively. Inset: a zoom-in view of the spectra. (b) 2D-spectro-temporal pattern of the frequency comb over 100-μs observation. Inset: a zoom-in view of the spectral pattern.

experiment, which makes the finer waveform structure that appeared in the simulation unable to be resolved in the experiment. From the perspective of space-time duality, these complicated temporal structures (time lens off) can be understood as
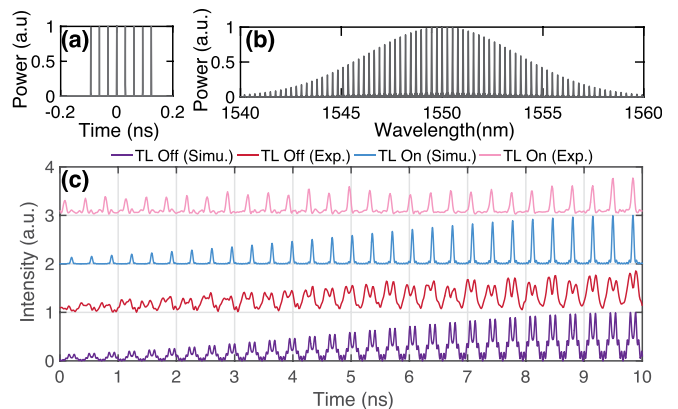

FIG. 5. Numerical simulation and experimental observation of 32.4-GHz frequency comb pulses passing through the system. (a) Simulated temporal waveform of 8 comb pulses at the time gate. (b) Simulated comb spectrum of (a). (c) Simulation results and the experimental observation of temporal waveforms at the system output when the time lens is turned on/off. TL, time lens.

the Fresnel (near-field) diffraction pattern of the gated input signal at a given propagation distance in the temporal domain. It is worth noting that although the comb pulses are temporally stretched after propagating through the dispersive media, given the time gate of 250-ps, the GDD provided by the DCF is far from enough to satisfy the temporal far-field diffraction approximation.[10] As a result, the temporal waveform at the system output does not resemble its spectral profile. Although this can be easily solved by further using a dispersive medium with a much larger GDD, the large GDD would inevitably lead to a much broader temporal waveform and hence require a much larger time window at the system output, which causes significant degradation of the system's repetition rate. Therefore, to enable a high-speed measurement, time lens focusing should be adopted compared with temporal far-field diffraction (i.e., DFT) for performing optical Fourier transform.

Compared with the PASTA system which utilizes an optical parametric process to generate the time lens, the proposed system is able to provide a wider spectral measurement range. However, it should be acknowledged that the PASTA system can offer a much wider time lens aperture and a much stronger time lens focusing (a 1-ns pulse was compressed to 50-ps in Ref. 18). Consequently, the PASTA system serves as a better fit for measuring the frequency comb with smaller comb spacing, where a larger time aperture is required to produce a clear comb spectrum. Nevertheless, we point out that the time lens focusing performance of the EO system is ultimately restricted by the available modulation depth of the phase modulator. Inspiringly, recent advance in the electro-optic phase modulator has reported a highly efficient design that can provide an ultralow V_π of 210 mV,[32] which is merely 1/15 of the V_π in this experiment. Therefore, we expect the performance of our system to be further enhanced with the development of the EO modulator.

In conclusion, a broadband real-time spectrum analysis technique based on a gating-assisted electro-optic time lens has been proposed. A spectral measurement range of more than 70-nm is achieved with the resolution of 42.5-pm at a repetition rate of 10-MHz. Its performance in applications is further verified by the dynamic spectral observation of lasing wavelength sweeping of a FDML and a 32.4-GHz frequency comb. With its broadband performance and repetition-rate tunability, we expect the proposed technique to be applied to provide real-time spectral analysis for widespread applications.

REFERENCES

[1] P. M. Kraus, M. Zürch, S. K. Cushing, D. M. Neumark, and S. R. Leone, Nat. Rev. Chem. **2**, 82 (2018).
[2] R. E. F. Silva, I. V. Blinov, A. N. Rubtsov, O. Smirnova, and M. Ivanov, Nat. Photonics **12**, 266 (2018).
[3] G. Ycas, F. R. Giorgetta, E. Baumann, I. Coddington, D. Herman, S. A. Diddams, and N. R. Newbury, Nat. Photonics **12**, 202 (2018).
[4] Y. Tong, L. Chan, and H. Tsang, Electron. Lett. **33**, 983 (1997).
[5] M. A. Muriel, J. Azaña, and A. Carballar, Opt. Lett. **24**, 1 (1999).
[6] P. Kelkar, F. Coppinger, A. Bhushan, and B. Jalali, Electron. Lett. **35**, 1661 (1999).
[7] A. F. Runge, N. G. Broderick, and M. Erkintalo, Optica **2**, 36 (2015).
[8] G. Herink, F. Kurtz, B. Jalali, D. Solli, and C. Ropers, Science **356**, 50 (2017).
[9] Y. Wei, B. Li, X. Wei, Y. Yu, and K. K. Y. Wong, Appl. Phys. Lett. **112**, 081104 (2018).
[10] J. Azaña and M. A. Muriel, IEEE J. Quantum Electron. **36**, 517 (2000).
[11] K. Goda, D. R. Solli, K. K. Tsia, and B. Jalali, Phys. Rev. A **80**, 043821 (2009).
[12] B. H. Kolner, IEEE J. Quantum Electron. **30**, 1951 (1994).
[13] R. Salem, M. A. Foster, and A. L. Gaeta, Adv. Opt. Photonics **5**, 274 (2013).
[14] T. Jannson, Opt. Lett. **8**, 232 (1983).
[15] N. Berger, B. Levit, S. Atkins, and B. Fischer, Electron. Lett. **36**, 1644 (2000).
[16] Y. Zheng, J. Li, Y. Dai, F. Yin, and K. Xu, Opt. Lett. **43**, 194 (2018).
[17] C. Zhang, J. Xu, P. Chui, and K. K. Y. Wong, Sci. Rep. **3**, 2064 (2013).
[18] B. Li, Y. Wei, J. Kang, C. Zhang, and K. K. Y. Wong, Opt. Lett. **43**, 1922 (2018).
[19] C. Zhang, B. Li, and K. K.-Y. Wong, IEEE J. Sel. Top. Quantum Electron. **22**, 295 (2016).
[20] X. Wei, B. Li, Y. Yu, C. Zhang, K. K. Tsia, and K. K. Wong, Opt. Express **25**, 29098 (2017).
[21] D. R. Solli, J. Chou, and B. Jalali, Nat. Photonics **2**, 48 (2008).
[22] J. van Howe, J. Hansryd, and C. Xu, Opt. Lett. **29**, 1470 (2004).
[23] B. Li, X. Wei, S. Tan, J. Kang, and K. K. Y. Wong, Opt. Lett. **41**, 1562 (2016).
[24] H. Zhou, L. Chen, X. Zhou, C. Zhang, K. K. Y. Wong, and X. Zhang, in Conference on Lasers and Electro-Optics (Optical Society of America, 2017), JTh2A.122.
[25] S. Namiki and Y. Emori, IEEE J. Sel. Top. Quantum Electron. **7**, 3 (2001).
[26] R. Huber, M. Wojtkowski, and J. Fujimoto, Opt. Express **14**, 3225 (2006).
[27] C. M. Eigenwillig, B. R. Biedermann, G. Palte, and R. Huber, Opt. Express **16**, 8916 (2008).
[28] Y. K. Chembo, D. V. Strekalov, and N. Yu, Phys. Rev. Lett. **104**, 103902 (2010).
[29] B. Li, S.-W. Huang, Y. Li, C. W. Wong, and K. K. Y. Wong, Nat. Commun. **8**, 61 (2017).
[30] B. Yao, S.-W. Huang, Y. Liu, A. K. Vinod, C. Choi, M. Hoff, Y. Li, M. Yu, Z. Feng, D.-L. Kwong, Y. Huang, Y. Rao, X. Duan, and C. W. Wong, Nature **558**, 410–414 (2018).
[31] X. Yi, Q.-F. Yang, K. Y. Yang, and K. Vahala, Nat. Commun. **9**, 3565 (2018).
[32] C. Kieninger, Y. Kutuvantavida, D. L. Elder, S. Wolf, H. Zwickel, M. Blaicher, J. N. Kemal, M. Lauermann, S. Randel, and W. Freude, Optica **5**, 739 (2018).